

Tracing the asymmetry in the envelope around the carbon star C IT 6

Dinh-V-Trung¹ and Jeremy Lin

trung@asiaa.sinica.edu.tw, jlim@asiaa.sinica.edu.tw

Institute of Astronomy and Astrophysics, Academia Sinica

P.O. Box 23-141, Taipei 10617, Taiwan.

Received _____; accepted _____

¹On leave from Center for Quantum Electronics, Institute of Physics

Vietnamese Academy of Science and Technology, 10 Dao Tan, Ba Dinh, Hanoi, Vietnam

A B S T R A C T

We present high angular resolution observations of HC_3N $J=5\{4$ line and 7 mm continuum emission from the extreme carbon star C IT 6. We find that the 7 mm continuum emission is unresolved and has a flux consistent with black-body thermal radiation from the central star. The HC_3N $J=5\{4$ line emission originates from an asymmetric and clumpy expanding envelope comprising two separate shells of HC_3N $J=5\{4$ emission: (i) a faint outer shell that is nearly spherical which has a radius of 8° ; and (ii) a thick and incomplete inner shell that resembles a one-arm spiral starting at or close to the central star and extending out to a radius of about 5° . Our observations therefore suggest that the mass loss from C IT 6 is strongly modulated with time and highly anisotropic. Furthermore, a comparison between the data and our excitation modelling results suggests an unusually high abundance of HC_3N in its envelope. We discuss the possibility that the envelope might be shaped by the presence of a previously suggested possible binary companion. The abundance of HC_3N may be enhanced in spiral shocks produced by the interaction between the circumstellar envelope of C IT 6 and its companion star.

Subject headings: circumstellar matter: | ISM : molecules | stars: AGB and post-AGB | stars: individual (C IT 6) | stars: mass loss

1. Introduction

The circumstellar envelope around carbon-rich asymptotic giant branch (AGB) stars is well known to be the site of very active photochemistry and hence a rich source of molecular emission lines. The prime example is the massive carbon rich circumstellar envelope of

the nearby AGB star IRC+10216 (CW Leo), where more than 50 molecular species have been detected. Many spectral line surveys in the millimeter wavelength range have been conducted toward IRC+10216 (He et al. 2008, Cernicharo & Guélin 2000, Kawaguchi et al. 1995). These surveys show that the emission lines from cyanopolyynes molecules such as HC_3N and HC_5N are very prominent in the millimeter wavelengths. Interferometric observations of HC_3N lines in the 3-mm band by Bieging & Tafalla 1994 with BM A and by Guélin et al. (2000) with the IRAM PdBI show that the cyanopolyynes molecules have a hollow shell distribution, consistent with the predictions of chemical models for a carbon rich circumstellar envelope (Cherchneff et al. 1993, Millar & Herbst 1994, Millar et al. 2000, Brown & Millar 2003). Even higher angular resolution observations of HC_3N $J=5\{4$ and HC_5N $J=16\{15$ lines in the 7 mm band by Dinh-V-Trung & Lim (2008) with the Very Large Array (VLA), which are detectable over a more radially extended region, revealed the presence of a number of incomplete shells representing different episodes of mass loss enhancement from the central AGB star. These observations show that the emission of cyanopolyynes molecules can be used to trace the small scale structures of the envelope.

The spatial distribution of cyanopolyynes molecules in the circumstellar envelope around other carbon-rich stars has been much less studied at high angular resolution. Here, we present observations of the HC_3N $J=5\{4$ line around C IT 6 (RW LMi, GL 1403 or IRAS 10131+3049) with the VLA. C IT 6, a semiregular variable, is an extreme carbon star enshrouded in a massive molecular envelope, very similar to the archetypical carbon star IRC+10216. It has a pulsation period of 640 days, which, based on the period-luminosity relation for evolved stars, translates to a distance of ~ 400 pc (Cohen 1980 and Cohen & Hitchon 1996). For easy comparison with previous work, we will adopt a distance of 440 pc for C IT 6, which is similar to that used by Schoeier et al. (2002). High resolution optical imaging of Schmidtb et al. (2002) shows a series of arcs in the optical reflection nebula around C IT 6, within $2''$ of the star. These arcs comprise the density enhancement in the

envelope and indicate variations of mass loss on the scale of several hundred years. Such dusty arcs have previously been seen in a number of other circumstellar envelopes and AGB and post-AGB stars such as IRC+10216 (Mauron & Huggins 1999), the Egg nebula (Sahai et al. 1998) and some proto-planetary nebulae (Hrivnak et al. 2001).

Interferometric observations of CO $J=1\{0$ line by Neri et al. (1998) and Meixner et al. (1998) at angular resolution of $3''\{6''$ reveal a bright central core surrounded by a more diffuse but roughly spherical envelope, expanding at a velocity $\sim 18 \text{ km s}^{-1}$. Using sophisticated radiative transfer models, Schoeier & Olofsson (2001) and Schoeier et al. (2002) estimated a mass loss rate of $5 \times 10^{-6} M_{\odot} \text{ yr}^{-1}$ for CIT 6 by fitting the strength of CO rotational lines. They also noted that a more satisfactory match between model predictions and observations could be obtained if mass loss variation is introduced into the model. Teyssier et al. (2006) also reached similar conclusion from modelling the single dish observations of CO rotational lines in CIT 6. Apart from CO, several other molecules have been detected in CIT 6, including cyanopolynes (Zhang et al. 2008). The overall chemical makeup of its envelope is similar to that of the archetypical carbon rich envelope IRC+10216, with the exception of enhanced SiC₂ and cyanopolyyne emissions. The distributions of other molecules such as the cyanopolynes (HC₃N and HC₅N) and HCN and CN have been mapped at an angular resolution of about $3''$ by Lindqvist et al. (2000). Only the emission of cyanogen radical CN was well resolved into an incomplete and elongated expanding shell.

In this paper we present our high angular resolution observations of HC₃N $J=5\{4$ emission from CIT 6 obtained with the Very Large Array (VLA²). The observations allow us to probe the structure of the envelope at arcsec scale or $\sim 6 \times 10^{15} \text{ cm}$.

²The VLA is a facility of the National Radio Astronomy Observatory, which is operated by Associated Universities, Inc., under contract with the National Science Foundation

2. Observation

We observe C II 6 on 2003 April 13, using the Very Large Array (VLA) in its most compact configuration. The telescope was pointed at $\alpha_{2000}=10^{\text{h}}16^{\text{m}}02.27^{\text{s}}$, $\delta_{2000}=30^{\circ}34'18.6''$, the location of the star as listed in the SIMBAD database (Loup et al. 1993). The rest frequency of the HC_3N $J=5-4$ line as compiled by the Lovas/NIST database (Lovas 2004) is 45.490316 GHz. To observe this line we configured the VLA correlator in the 2AC mode with 6.25 MHz bandwidth over 64 channels, thus providing a velocity resolution of 0.65 km s^{-1} per channel over a useful velocity coverage of $\sim 40 \text{ km s}^{-1}$. The total on-source time is about 1 hour. We monitored the nearby quasar 0958+324 at frequent intervals to correct for the antennas gain variations caused primarily by atmospheric fluctuations. The stronger quasars 0927+390 and 1229+020 were used to correct for the shape of the bandpass and its variation with time. The absolute flux scale of our observations was determined from observation of standard quasar 3C 147 (0542+498).

We edited and calibrated the raw visibilities using the AIPS data reduction package. The calibrated visibilities were then Fourier transformed to form the DRTY images. We employed the robust weighting to obtain a satisfactory compromise between angular resolution and sensitivity. The DRTY images were deconvolved using normal clean algorithm implemented in AIPS, providing a synthesized beam of $1.5'' \times 1.4''$ at position angle $\text{PA} = 24.8^\circ$. The rms noise level in our channel maps of HC_3N $J=5-4$ emission is $6.7 \text{ mJy beam}^{-1}$ in each velocity channel of 2.6 km s^{-1} . The corresponding conversion factor between the brightness temperature of the HC_3N $J=5-4$ emission and the flux density is 4 mJy/K .

We also configured the VLA in normal continuum mode at 7 mm. The on source integration time for C II 6 is about 10 minutes. The same calibrators as above were used for complex gain and absolute flux density calibration. We processed the continuum data in

the same manner as the line data. The resulting synthesized beam is $2''.3 \times 1''.6$ at position angle $PA = 75^\circ$. The rms noise level of the continuum map is $0.4 \text{ mJy beam}^{-1}$.

3. Results

We detected an unresolved continuum source at 7 mm with a flux density of $2.4 \pm 0.4 \text{ mJy}$ at 10h16m 02.27s and 30d34m 19.1s. This is coincident within the errors (about $0.4''$) with the position of an unresolved continuum source at 3 mm with a flux of $8 \pm 0.4 \text{ mJy}$ detected by Lindqvist et al. (2000). The spectral index between 7 mm and 3 mm is very close to 2 (i.e. $S \propto \nu^{-2}$), consistent with stellar black body radiation from presumably the central AGB star in CIT 6. At shorter wavelengths, the spectral index is larger with $S \propto \nu^{-3.1}$, indicating significant contribution from dust in the envelope around CIT 6 (Neri et al. 1998, Marshall et al. 1992).

Figure 1 shows the channel maps of the $\text{HC}_3\text{N } J=5\{4$ emission. Figure 2 shows the $\text{HC}_3\text{N } J=5\{4$ profile derived by integrating over a region where the emission is detected above 2σ level. The $\text{HC}_3\text{N } J=5\{4$ line has been previously observed by Fakasaku et al. (1994) with the Nobeyama 45m telescope, which has a primary beam of about $40''$ at FWHM. Using the main beam efficiency provided by Fakasaku et al. (1995), we estimate a conversion factor of 4 Jy/K, thus giving a peak flux density of about 1.7 Jy for the $\text{HC}_3\text{N } J=5\{4$ line. This is comparable to the peak flux density of 1.6 Jy measured in our observation (see Figure 2). Furthermore, the shape of the line profiles in both observations are also very similar, suggesting that our VLA observation has recovered most of the emission in the $\text{HC}_3\text{N } J=5\{4$ line present in the aforementioned single dish observation.

The channel maps of $\text{HC}_3\text{N } J=5\{4$ emission shows the usual pattern of an expanding envelope, with the emitting region being largest at the systemic velocity $V_{\text{LRS}} = 2 \text{ km s}^{-1}$.

and becoming progressively more compact at large blueshifted and redshifted velocities. From the velocity range covered by the emission in the channel maps we estimate that the expansion velocity of the HC_3N shell is about 17 km s^{-1} , which is in good agreement to the expansion velocity of 18 km s^{-1} inferred from previous CO observations (Neri et al. 1998, Meixner et al. 1998). Unlike the well-defined hollow shell structure seen in $\text{HC}_3\text{N } J=5\{4$ and $\text{HC}_5\text{N } J=16\{15$ for IRC+10216 (Dinh-V-Trung & Lim 2008), however, the spatial distribution of $\text{HC}_3\text{N } J=5\{4$ emission in CIT 6 is much more complex. In the velocity channel at $V_{\text{LSR}} = 13.5 \text{ km s}^{-1}$, the emission appears roughly spherically symmetric. In the velocity channels between 17.4 to 8.3 km s^{-1} , however, the emission resembles an incomplete shell with a mostly complete eastern portion whereas the western part is missing. Previous observations of $\text{HC}_3\text{N } J=10\{9$ line at lower angular resolution of $3''$ by Lindqvist et al. (2000) also show a lopsided envelope that is strongly enhanced in the eastern portion together with significant emission at the stellar position.

To show more clearly the structures within the expanding envelope of CIT 6, we integrate the line intensity spanning velocities 7.1 to 5.7 km s^{-1} , namely the 6 velocity channels straddling the systemic velocity. The resulting integrated intensity map is shown in Figure 3. The envelope clearly does not resemble a spherical expanding hollow shell expected for molecules such as HC_3N . Instead, starting from the stellar position, the brightest portion of the emission extends to the south, curls to the east and north, and then curls again to the west and south, thus creating a structure resembling a one-arm spiral. In the channel maps, this spiral structure can be most clearly seen at the systemic velocity of 2 km s^{-1} and the adjacent channel at 0.6 km s^{-1} . Such a spiral distribution in molecular emission has never been seen before in any circumstellar envelope.

Beyond the outermost radius of the one-armed spiral, there is fainter emission tracing a nearly spherical shell with radius of $8''$. This shell can be seen, along with the one-armed

spiral in the channel maps between velocities of 3.2 and 5.7 km s^{-1} . The faint outer shell is more visible in the integrated intensity map shown in Figure 3. The outer shell appears to be centered on the central AGB star as indicated by its continuum emission at 7 mm and seems to be even more clumpy than the one-armed spiral. For clarity, we sketch the location and the outline of these two structures in Figure 4.

Using the conversion factor of 4 mJy/K we estimate that the brightness temperature of the $\text{HC}_3\text{N } J=5\{4$ emission in the channel maps around the systemic velocity (± 2 and 0.6 km s^{-1}) ranges from about 5 K to 12 K . We note that the measured brightness temperature is smaller but quite significant in comparison to the kinetic temperature of the molecular gas in the range 20 to 80 K expected from the modelling of the envelope of C II 6 (Schoeier et al. 2002, Dinh-V-Trung et al. 2008 in preparation), indicating that the optical depth in the $\text{HC}_3\text{N } J=5\{4$ line is significant if the line is close to thermalization.

4. Discussion

4.1. Comparison with previous observations

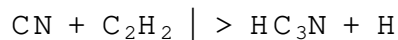
The existence of spatially distinct and incomplete molecular shells as traced by the $\text{HC}_3\text{N } J=5\{4$ emission again emphasizes the similarity between C II 6 and the archetypical carbon star IRC + 10216. In the later case, numerous incomplete expanding shells have been detected and linked to different episodes of mass loss enhancement from the central AGB star (Dinh-V-Trung & Lin 2008). In C II 6 the presence of the shells as well as the dust arcs seen in the optical (Schmidt et al. 2002), all point to previous episodes of mass loss enhancement. From the radius of the outer shell of 8 arcsec and an expansion velocity of 18 km s^{-1} , we estimate that the episode of mass loss that gave rise to this thin shell happened about 10^3 years ago. The inner shell, which resembles a one-armed spiral, spans radii of

1^{\odot} to 5^{\odot} . That corresponds to a time scale between 120 to 600 years.

High resolution optical images of Schmidt et al. (2002) show a bipolar morphology for the nebula around the envelope. Because the bipolar morphology is typical of post-AGB objects such as the Egg nebula or CRL 618, they suggested that CIT 6 has reached the end of the AGB phase. Our data, however, do not show any evidence of bipolar morphology in the molecular envelope. The bipolar morphology seen in the optical is therefore likely an illumination effect due to the peculiar distribution of the material close to star. For example, a spherical envelope with its polar caps removed will allow starlight to escape more easily in the polar directions thus creating an apparent bipolar morphology in the reflection nebula.

4.2. Excitation of HC_3N

The existence of HC_3N $J=5\{4$ emission close to the central star of CIT 6 is surprising given the commonly accepted formation pathway for HC_3N and also the excitation conditions in the envelope. Chemical models for carbon rich circum stellar envelope predict that HC_3N molecules form from the reaction between CN, which is a photodissociation product of parent molecule HCN, and acetylene C_2H_2 :



Therefore, very few HC_3N molecules are expected to exist in the inner region of the envelope as few interstellar UV photons can penetrate into the inner region to produce CN radicals through photodissociation of HCN. That conclusion can be seen in the predictions of chemical models of Cherchne et al. (1993), Millar & Herbst (1994) and Millar et al. (2000). Observations of high-lying transitions of HC_3N observations by Audinos et al. (1994), however, suggest that the abundance of HC_3N in the inner region of the envelope around the archetypical carbon star IRC+10216 is quite significant, nearly an order of

magnitude higher than predicted by chemical models.

Do we expect to observe the $\text{HC}_3\text{N } J=5\{4$ line in the inner region of the envelope? The answer is likely negative because the higher gas density and kinetic temperature in the inner region can easily lead to the excitation of HC_3N to higher rotational levels. That effectively reduces the optical depth, and consequently, the intensity of low lying rotational transitions. As a result, only high lying transitions of HC_3N might be detected in the inner region. Observationally, high lying transitions of HC_3N up to $J=29\{28$ have been detected in the spectral line survey toward CIT 6 of Zhang et al. (2008). Based on this simple argument, the existence of low lying $\text{HC}_3\text{N } J=5\{4$ emission close to the central star is not expected, except when the abundance of HC_3N is extremely high.

To check the above argument more quantitatively and to explore an alternative explanation for the observed $\text{HC}_3\text{N } J=5\{4$ emission close to the AGB star of CIT 6, we have performed the excitation calculations for HC_3N molecules in the envelope of CIT 6. The calculations were carried out using the large velocity gradient (LVG) approximation, which is justified for the case of CIT 6 where the expansion velocity ($\sim 18 \text{ km s}^{-1}$) is large. We use the HC_3N molecular data compiled by Langer & Lovas (1978) and Umemura et al. (1982). We include in our model the radiative excitation of the molecule due to IR pumping through the ν_5 bending vibrational state. As suggested by Bieging & Tafalla (1993), this mode is strongest and its wavelength is close to the peak of the continuum spectrum of IRC+10216 and also CIT 6. Therefore the ν_5 bending mode should play a dominant role in the radiative excitation process. We include all rotational levels in the ground state and $\nu_5=1$ vibrational state up to $J=30$. Because the Q-branch ro-vibrational transitions do not effectively contribute to the radiative excitation of the HC_3N molecule, we consider only transitions in the P and R-branches in our model. We also adopt the same dipole moment of 0.18 Debye for the vibrational transition between ν_5 state and the ground state as used

in Audinos et al. (1994). The collisional cross sections between HC_3N and H_2 are assumed to follow the prescription of Deguchi et al. (1984). From detailed modelling of the structure of the envelope (Dinh-V-Trung et al. 2008 in preparation, Schoeier et al. 2002), the mass loss rate of C II 6 is found to be $5 \times 10^{-6} M_\odot \text{ yr}^{-1}$. The gas temperature as a function of radial distance in the envelope as derived from our modelling results can be approximated as $T_K(r) = 33 \text{ K} (r/3 \times 10^{16} \text{ cm})^{-0.6}$. We note that the kinetic temperature in the envelope of C II 6 is significantly lower in comparison to that in IRC+10216 (Bieging & Tafalla 1993, Audinos et al. 1994). Because both C II 6 and IRC+10216 share very similar properties such as the total luminosity, the overall shape of the SED (Lindqvist et al. 2000), we follow Bieging & Tafalla (1993) and adopt a blackbody IR continuum source having $5.1 \times 10^{14} \text{ cm}$ in radius and a temperature of 600 K.

We adopt an abundance of HC_3N with respect to H_2 of the form $f_{\text{HC}_3\text{N}} = f_0 \exp\{[4 \ln 2 (r/r_0)^2 / \text{FWHM}^2]\}$, where f_0 is the peak abundance, r_0 is the radius of the peak abundance and FWHM is the full width at half maximum of the radial distribution. This functional form of the abundance distribution is similar to that used by Bieging & Tafalla (1993) to model the $\text{HC}_3\text{N } J=10\{9$ line in the envelope of IRC+10216. Because the $\text{HC}_3\text{N } J=5\{4$ emission in C II 6 exists over a large range of radii, between $1''$ to $8''$, we use a representative value $r_0 = 4 \times 10^{16} \text{ cm}$ or $6''$ in angular distance.

In order to reproduce the measured brightness temperature of $\text{HC}_3\text{N } J=5\{4$ line in C II 6, which is in the range of 5–12 K for channel maps around the systemic velocity, we find that a peak abundance of $f_0 = 5 \times 10^{-6}$ is needed. In Figure 5 we show the results of our model. For the case with $\text{FWHM} = 2 \times 10^{16} \text{ cm}$, which reproduces the broad distribution of HC_3N derived by Audinos et al. (1994) for IRC+10216, the predicted peak brightness temperature of $\text{HC}_3\text{N } J=5\{4$ line is 10 K, comparable to the aforementioned observed brightness temperature. The predicted brightness temperature is found to peak at a smaller

radius in comparison to the underlying abundance distribution of HC_3N . That can be easily understood because the location of the peak in brightness temperature is determined not just by the abundance but by the overall balance between gas density, the abundance of HC_3N and the gas temperature. At the radii between $1''$ to $2''$, because of very low abundance of HC_3N , the predicted brightness temperature is almost zero. To reproduce the brightness temperature of ~ 5 K seen close to the central AGB star in the channel maps around the systemic velocity, we need to broaden the abundance distribution of HC_3N by increasing the parameter FWHM to 3.5×10^{16} cm. The abundance of HC_3N in the inner envelope is then increased by more than two orders of magnitude as shown in Figure 4. The predicted brightness temperature between the radii of $1''$ to $2''$ is now comparable to the observed value.

The qualitative calculations presented here clearly indicate that the abundance of HC_3N in the envelope of CIT 6 is significantly higher in comparison to that found in the archetypical carbon rich envelope of IRC + 10216, which has a peak HC_3N abundance of $f_0 = 10^{-6}$ derived by Audinos et al. (1994). The especially elevated abundance in the inner envelope close to the central AGB star of CIT 6 can not easily be explained by the current chemical models of carbon rich envelopes.

4.3. The binary hypothesis

The inferred high abundance of HC_3N in the envelope around CIT 6, especially in the inner region close to the star and the unusual spatial distribution of HC_3N $J=5-4$ emission resembling a one-arm spiral suggest that mechanisms other than photochemistry might be at work to form the HC_3N molecules.

Guelin et al. (1999) noted that many molecular species in IRC + 10216 are co-spatial

even though they are predicted by chemical models (Cherchneff et al. 1993, Millar et al. 2000) to form at different radial distances. The similar spatial distribution of different molecular species indicates that the molecules are all formed in a very short timescale, of the order of hundred of years. They suggest that other mechanisms such as desorption from dust grain or the release from grain surface due to shocks might be responsible for the formation of molecules in carbon rich circum stellar envelopes.

Binary companions around AGB stars have been suggested to play important role in shaping the structure and influencing the wind dynamics within the circum stellar envelope. Indeed, in the hydrodynamic simulations of Mastromaros & Morris (1999), Edgar et al. (2008), the interaction with a binary companion can induce spiral shocks and enhance the density structure in the envelope around a mass losing star. The density structure in the envelope is predicted to resembles a one-arm spiral (see Figures 1 & 2 in Edgar et al. 2008). Such spiral structure has recently been seen in the high resolution optical image of an extreme carbon star CRL 3068 (Morris et al. 2006, Maun & Huggins 2006). The elevated density and temperature expected in the spiral shocks (Edgar et al. 2008) might be conducive to the formation of large carbon chain molecules including HC_3N as suggested by Guelin et al. (1999).

In the case of CIT 6, optical spectropolarimetric observations of Schmidt et al. (2002) showed that its optical spectrum possesses a strong and featureless blue continuum excess. They attributed the blue continuum excess to the presence of a companion star of spectral type A-F buried in the envelope. Thus the high asymmetric envelope of CIT 6 as traced by the HC_3N emission might be caused by the binary companion. Assuming that the HC_3N emission traces the spiral shock produced by the companion, the period of the binary system might be estimated from shape of the one-arm spiral. As can be seen from the sketch of the structures in the envelope around CIT 6 (see Figure 4), the spiral makes

almost a complete turn, starting from the central AGB star in the South-West quadrant and ending in the North-West quadrant at the radial distance of about $5''$. The dynamical timescale corresponding to the inter-arm spacing of the spiral shock is directly related to the recession motion of the AGB star, i.e. the orbital period of the binary system (Mastrodomos & Morris 1999). Using the expansion velocity of 18 km s^{-1} and the adopted distance of 440 pc, the orbital period of the binary system is about 600 years. The long orbital period indicates that the companion must be in a wide orbit around the AGB star (the orbital separation is about 70 au if the primary AGB star has a mass of $1 M_{\odot}$). The estimate of orbital period for the binary system in CIT 6 is comparable to that (830 years) inferred by Maun & Huggins (2006) for the binary system in CRL 3068. Based on this argument, we think that the hypothesis of a binary system in CIT 6 is plausible as it could naturally account for the spatial distribution and the high abundance of HC_3N as seen in our observations. Future high angular resolution observations of dense and warm gas tracers such as high J transition of CO or HCN molecules will tell whether the spiral shock induced by the binary companion really exists within the envelope of CIT 6.

5. Conclusion

We have imaged at high angular resolution the distribution of $\text{HC}_3\text{N } J=5\{4$ emission from the envelope around carbon star CIT 6. We found that the emission of $\text{HC}_3\text{N } J=5\{4$ traces (1) a faint outer spherical shell located at a radial distance of 8 arcsec and centered at the position of the AGB star CIT 6 revealed by the detection of 7 mm continuum emission. (2) a thick and incomplete inner shell resembling a one-arm spiral. The presence of multiple shells in CIT 6 suggests that the mass loss from this star is highly anisotropic and episodic. From excitation modelling of HC_3N molecules we inferred that the abundance of HC_3N is unusually high in CIT 6 in comparison to the well known carbon star IRC+10216.

We suggest that the observed spatial distribution of the emission and the inferred high abundance of HC_3N might be caused by the presence of a binary companion in a wide orbit around C II 6.

We thank the VLA staff for their help with the observations. This research has made use of NASA's Astrophysics Data System Bibliographic Services and the SIMBAD database, operated at CDS, Strasbourg, France.

R E F E R E N C E S

- Audinos, P., Kahane, C., Lucas, R., 1994, *A & A*, 287, L5
- Biegging, J.H., Nguyen-Q Rieu, 1989, *ApJ*, 343, L25
- Biegging, J.H., Tafalla, M., 1993, *AJ*, 105, 576
- Bond, H., 2000, in *ASP Conf. Ser. 199*, ed. J.H. Kastner, N. Soker, S. Rappaport (San Francisco: ASP), 33
- Brown, J., Millar, T.J., 2003, *MNRAS*, 339, 1041
- Cherchne, I., Glassgold, A.E., Mammon, G.A., 1993, *ApJ*, 410, 188
- Cohen, M., 1980, *ApJ*, 238, L81
- Cohen, M., Hitchon, K., 1996, *AJ*, 111, 962
- Deguchi, S., Nakada, Y., Onaka, T., Uyemura, M., 1979, *PASJ* 31, 105
- Deguchi, S., Uyemura, M., 1984, *ApJ* 285, 153
- Dinh-V-Trung, Lin, J., 2008, *ApJ* 678, 303
- Edgar, R.G., Nordhaus, J., Blackman, E.G., Frank, A., 2008, *ApJ* 675, L101
- Fakasaku, S., Hirahara, Y., Masuda, A., et al., 1994, *ApJ* 437, 410
- Guelin, M., Neiningen, N., Lucas, R., Cernicharo, J., 1999, Ossenkopf V. ed. *The Physics and Chemistry of Interstellar Medium*, GCA-Verlag Herdecke, p. 326
- Hrivnak, B.J., Kwok, S., Su, K.Y.L., 2001, *AJ*, 121, 2775
- Kwok, S., Su, K.Y.L., Hrivnak, B.J., 1998, *ApJ*, 501, L117

- Lindqvist, M ., Schoeier, F L ., Lucas, R ., Olofsson, H ., 2000, A & A 361, 1036
- Larerty, W J., Lovas, F J., 1978, J.Phys.Chem .Ref.D ata 7, 441
- Lovas, F J., 2004, JPhysChem RefD ata, 33, 177
- Loup, C ., Forveille, T ., Omont, A ., Paul, JF ., 1993, A & A S 99, 291
- Marshall, C R ., Leahy, D A ., Kwok, S., 1992, PA SP, 104, 397
- Mastrodomos, N ., Morris, M ., 1999, ApJ 523, 357
- Mauron, N ., Huggins, P J., 2006, A & A 452, 257
- Meixner, M ., Campbell, M T ., Welch, JW ., Likkell, L ., 1998, ApJ 509, 392
- Millar, T J., Herbst, E ., 1994, A & A , 288, 561
- Millar, T J., Herbst, E ., Bettens, R P A ., 2000, M N R A S, 316, 195
- Morris, M ., Sahai, R ., Matthews, K ., Cheng, J., Lu, J., Claussen, M ., Sanchez Contreras, C ., 2006, Planetary nebulae in our galaxy and beyond, ed. Barlow , M J., Mendez, R H ., Proceedings of IAU 234, 469
- Neri, R ., Kahane, C ., Lucas, R ., Bujarrabal, V ., Loup, C ., 1998, A & A S, 130, 1
- Sahai, R ., et al. 1998, ApJ 493, 301
- Schoeier, F L ., Olofsson, H ., 2001, A & A , 368, 969
- Schoeier, F L ., Ryde, N ., Olofsson, H ., 2002, A & A 391, 577
- Schmidt, G D ., Hines, D C ., Swift, S., 2002, ApJ, 576, 429
- Terzian, Y ., Hajian, A R ., 2000, in A SP Conf. Ser. 199, ed. J.H . Kastner, N . Soker, S. Rappaport (San Francisco: A SP), 33

Teyssier, D ., Hemandez, R ., Bujarrabal, V ., Yoshida, H ., Phillips, T ., 2006, A & A 450, 167

Uyemura, M ., Deguchi, S ., Nakada, Y ., Onaka, T ., Chem . Soc. Japan 55, 384

Zhang, Y ., Kwok, S ., Dinh-V-Trung, 2008, astroph/808.3226

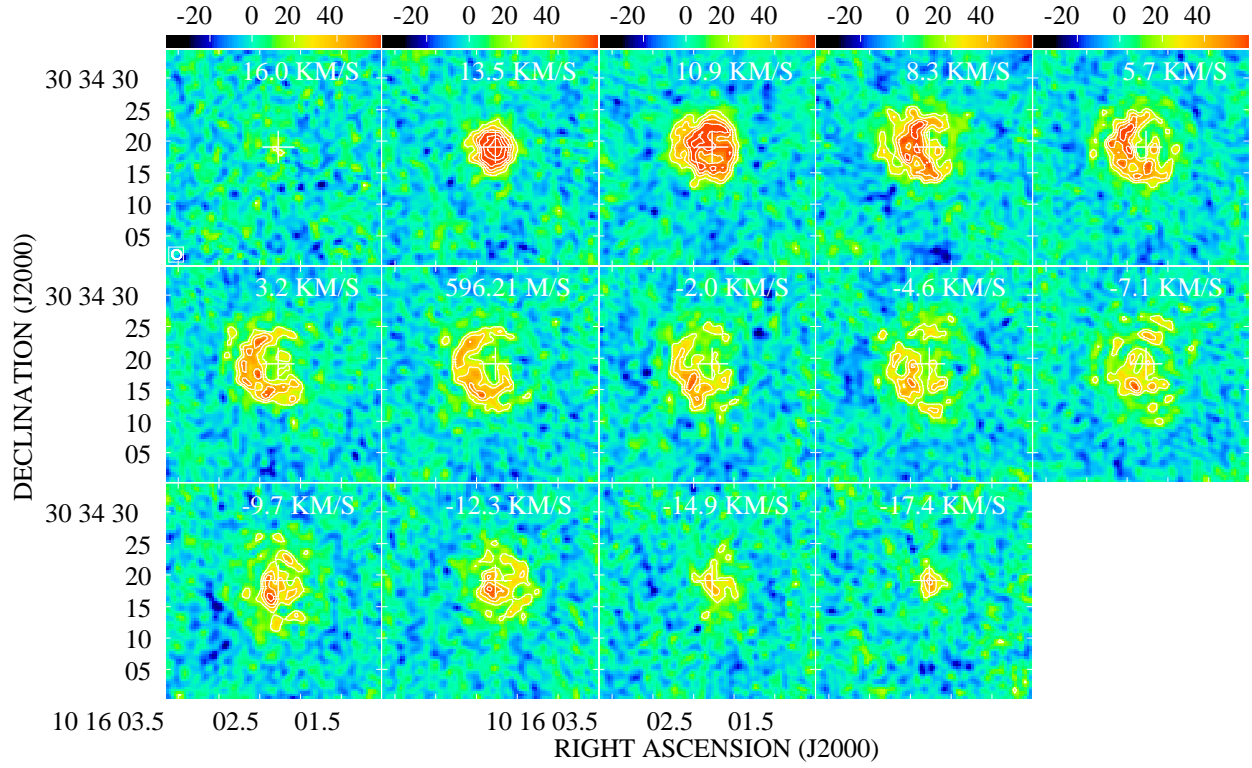


Fig. 1. Channel maps of the HC_3N $J=5-4$ emission (shown in false color and also in contours). The LSR velocity is indicated in the upper right of each frame. The contour levels are (3, 5, 7, 9, 12 and 15) with $\Delta = 6.7 \text{ mJy beam}^{-1}$. The synthesized beam is shown in lower left corner of the upper left frame. The corresponding conversion factor between the brightness temperature and flux density is 4 mJy/K .

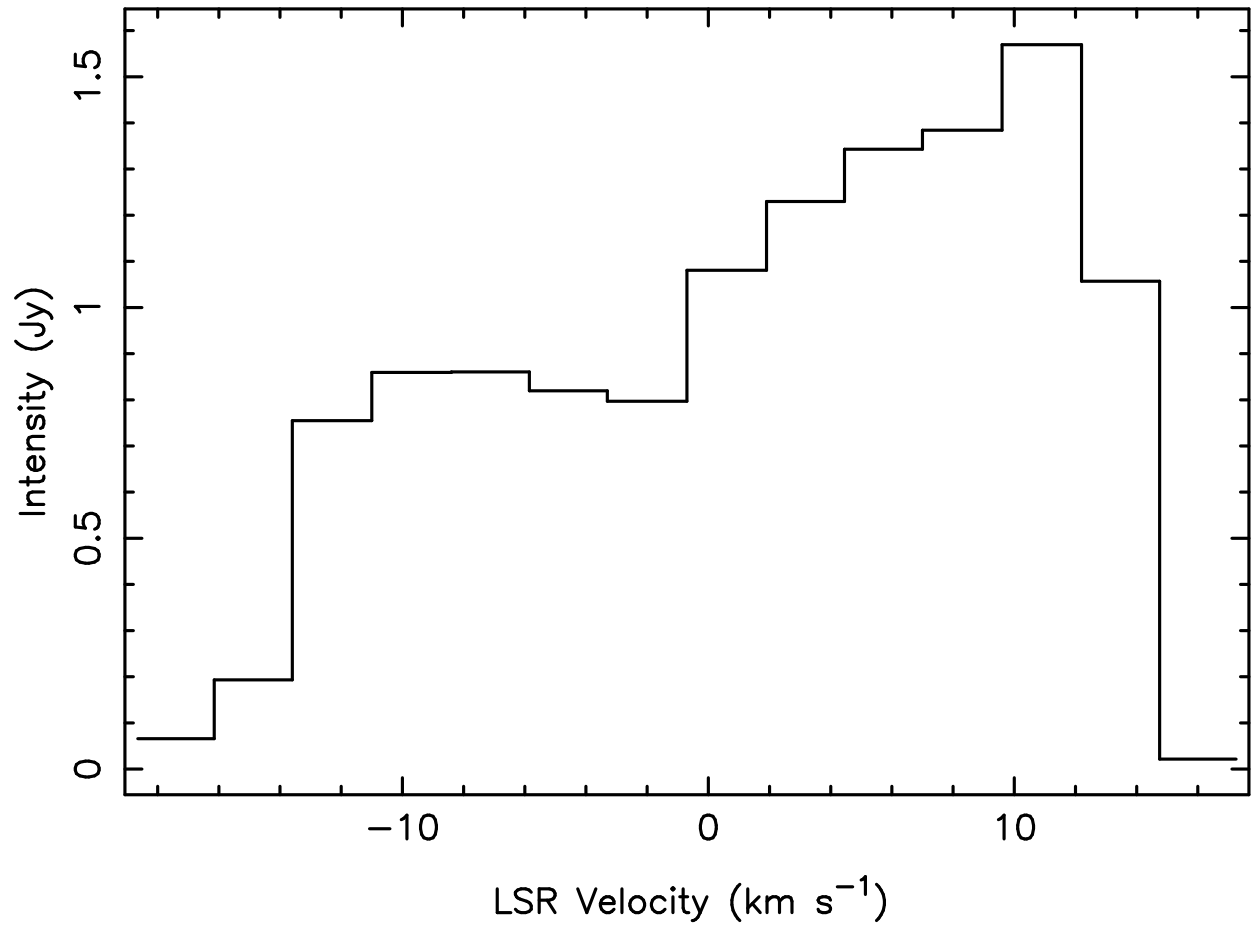


Fig. 2. Total intensity profile of the HC_3N $J=5-4$ line from C II 6.

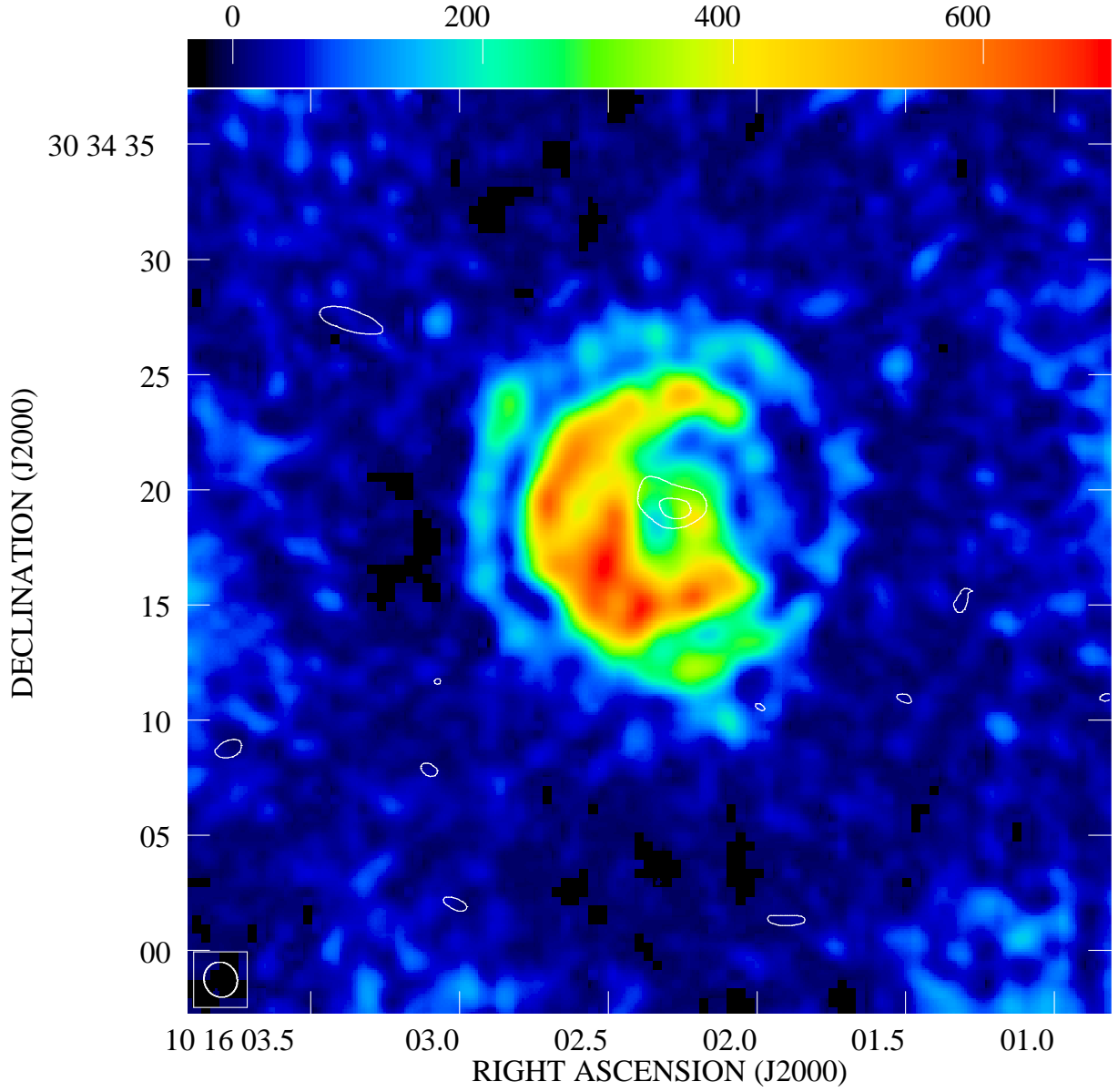


Fig. 3. The intensity of the HC_3N $J=5-4$ emission (shown in false color) integrated between velocity channels -7.1 to 5.7 km s^{-1} . The 7 mm continuum emission is also shown in contours. The contour levels are $1, 2 \text{ m Jy beam}^{-1}$. The intensity scale is $\text{m Jy km s}^{-1} / \text{beam}$. An outer nearly spherical shell and an incomplete shell resembling a one-arm spiral starting from the location of the central star indicated by the continuum emission are evident.

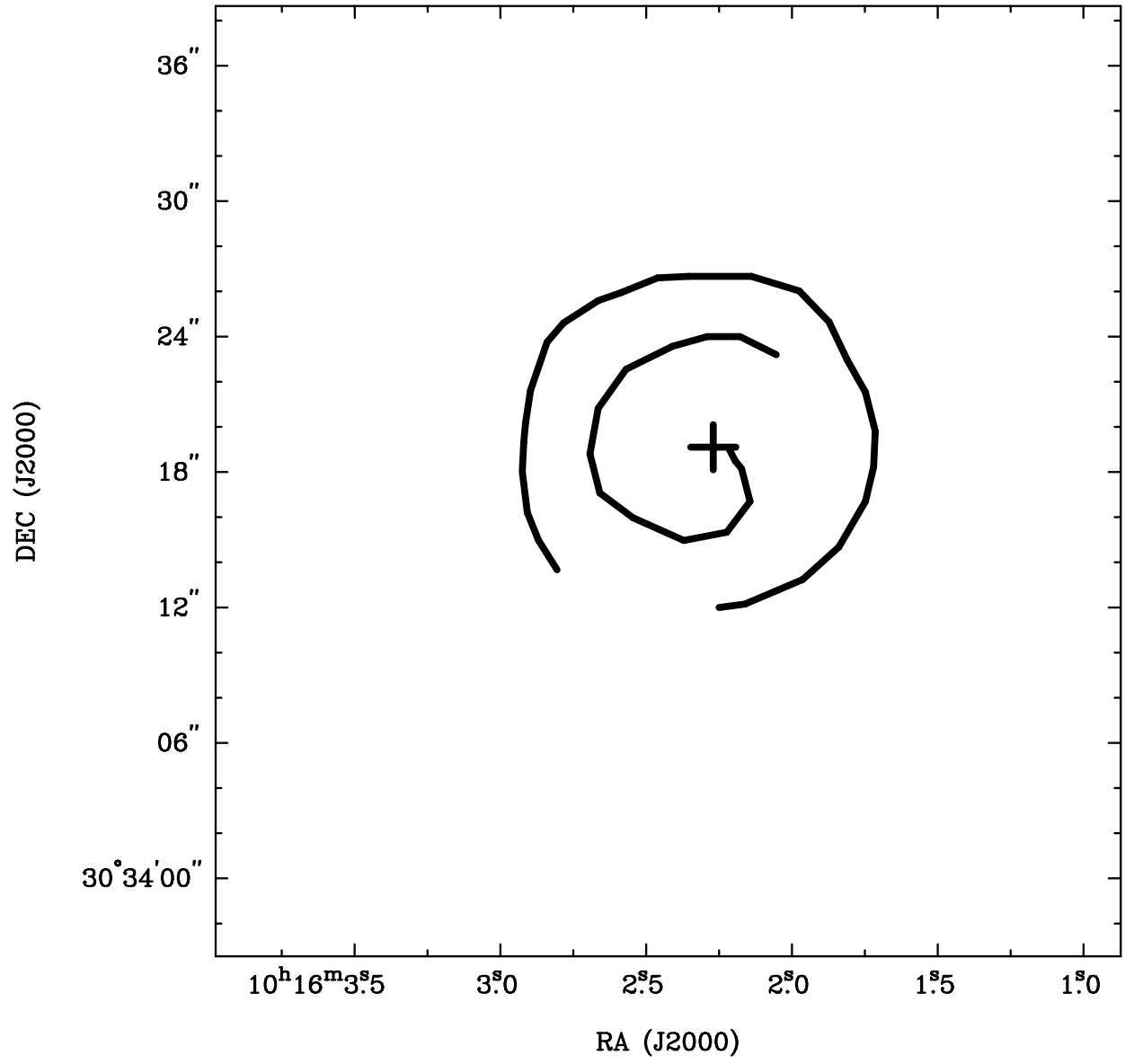


Fig. 4. Sketch of the outer spherical thin shell and the one-arm spiral in C II 6. The cross denotes the position of the AGB star.

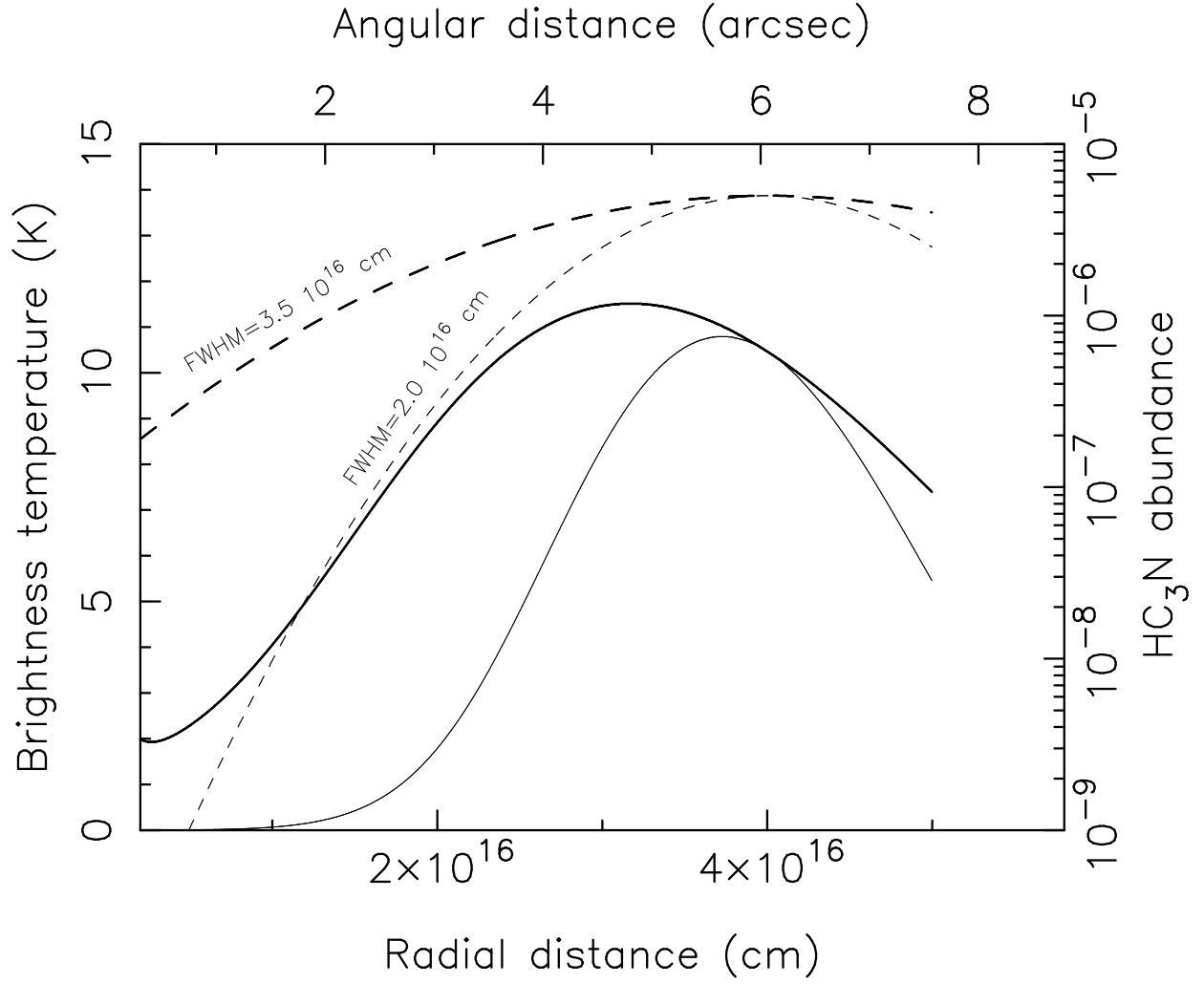


Fig. 5. Model calculation of the brightness temperature of $\text{HC}_3\text{N } J=5(4)$. The dashed lines represent the abundance of HC_3N with respect to H_2 in the envelope with different values of the FWHM parameter. The solid lines show the calculated brightness temperature. Thin lines represent the model with $\text{FWHM} = 2 \times 10^{16} \text{ cm}$ while the thick lines represent the model with broader distribution $\text{FWHM} = 3.5 \times 10^{16} \text{ cm}$, respectively.